PROC. OF JSCE,
No. 232, DEC. 1974

STRESS-DEFORMATION AND STRENGTH CHARACTERISTICS OF SOIL UNDER THREE DIFFERENT PRINCIPAL STRESSES

By Hajime MATSUOKA and Teruo NAKAI***

1. INTRODUCTION

The concept that the deformation of soil is governed by the shear-normal stress ratio on the mobilized plane of soil particles has already been discussed on the basis of the microscopic analysis of the behaviors of soil particles under shear.[1)~5)] This discussion originates in an idea that soil is one of the materials to which the frictional law in its broad sense of word applies. In the present paper, the authors expand the formerly proposed concept[2),4)] of three mobilized planes (compounded mobilized planes) among the three principal stress axes into a new postulate that a stress plane called "spatial mobilized plane" occurs in the three-dimensional stress space. Then, they propsse to verify, with various test data, the fact that stress-strain relationships of soil under three different principal stresses can uniquely be expressed by interpreting the relationships with respect to this plane. They also propose a new yield condition (failure criterion) of soil that soil yields when the shear-normal stress ratio on this plane has reached a fixed value.

2. SPATIAL MOBILIZED PLANE

It has been accepted that sliding of soil particles occurs to the greatest extent in the plane in which the ratio of shear stress to normal stress has the maximum value, i.e., the plane AC (cf. Fig. 1) called "mobilized plane" which is inclined by an angle of $(45°+\phi_{mo13}/2)$ (wherein $\phi_{mo13}=\sin^{-1}\{(\sigma_1-\sigma_3)/(\sigma_1+\sigma_3)\}$) from the direction of the minor principal stress. However, the direction in which the individual soil particles subjected to the three principal stresses σ_1, σ_2 and σ_3 slide is not necessarily parallel with the intermediate principal stress axis but is believed to be affected also by the intermediate principal stress σ_2. In this connection, there has been introduced a concept of "compounded mobilized planes"[2),4)] which is intended to explain the three-dimensional behaviors of soil particles by assuming other two

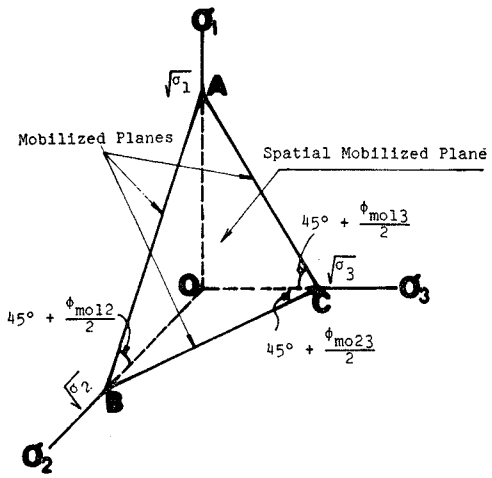

Fig. 1 Spatial mobilized plane and three mobilized planes in three principal stress space.

mobilized planes AB and BC among three principal stress axes. For the purpose of the present study, the authors introduce a stress plane ABC as the product of the combination of the three mobilized planes AB, BC and CA and give it a provisional designation of "spatial mobilized plane" (abbreviated as "SMP"). SMP, therefore, is believed to represent the resultant stress plane in which sliding of soil particles takes place to the greatest extent in the three principal stress space. The points at which SMP intersects the three principal stress axes are proportionate to the roots of the respective principal stresses as

* Dr. Eng., Assistant Professor, Disaster Prevention Research Institute, Kyoto University.
** M. Eng., Graduate Student, Kyoto University.

shown in Fig. 1, as indicated by the following equation.

$$\tan\left(45^\circ+\frac{\phi_{mo}{}_{ij}}{2}\right)=\sqrt{\frac{1+\sin\phi_{mo}{}_{ij}}{1-\sin\phi_{mo}{}_{ij}}}=\sqrt{\frac{\sigma_i}{\sigma_j}}\quad(i,j=1,2,3,\ i<j)\quad\cdots\cdots(1)$$

This resultant stress plane, therefore, is variable with possible change in the stresses. The direction consines (a_1, a_2, a_3) of the normal of SMP are expressed as follows.

$$a_1=\sqrt{\frac{J_3}{\sigma_1 J_2}},\quad a_2=\sqrt{\frac{J_3}{\sigma_2 J_2}},\quad a_3=\sqrt{\frac{J_3}{\sigma_3 J_2}}\quad\cdots\cdots(2)$$

wherein, J_1, J_2 and J_3 are the first, second and third stress invariants which are expressed by the following equations.

$$J_1=\sigma_1+\sigma_2+\sigma_3,\quad J_2=\sigma_1\sigma_2+\sigma_2\sigma_3+\sigma_3\sigma_1,\quad J_3=\sigma_1\sigma_2\sigma_3\quad\cdots\cdots(3)$$

Throughout this paper, the term "stress" shall invariably interpreted as representing "effective stress." In this paper, the various test data will be analyzed with consideration for the stress plane called "spatial mobilized plane (SMP)."

3. STRESS-STRAIN RELATIONSHIPS BASED ON SMP

The normal stress σ_N and the shear stress τ on the spatial mobilized plane (SMP) are expressed as follows:

$$\sigma_N=\sigma_1\cdot a_1^2+\sigma_2\cdot a_2^2+\sigma_3\cdot a_3^2=3J_3/J_2\quad\cdots\cdots(4)$$

$$\tau=\sqrt{(\sigma_1-\sigma_2)^2\cdot a_1^2\cdot a_2^2+(\sigma_2-\sigma_3)^2\cdot a_2^2\cdot a_3^2+(\sigma_3-\sigma_1)^2\cdot a_3^2\cdot a_1^2}=\frac{\sqrt{J_1J_2J_3-9J_3^2}}{J_2}\quad\cdots\cdots(5)$$

The shear-normal stress ratio (τ/σ_N) on the SMP, therefore, is given by the following equation.

$$\frac{\tau}{\sigma_N}=\sqrt{\frac{J_1J_2-9J_3}{9J_3}}\quad\cdots\cdots(6)$$

On the assumption that the direction of the principal stress and that of the principal strain increment are identical, the normal strain increment $d\epsilon_N$ and the shear strain increment $d\gamma$ on the SMP can be given by the following expressions.

$$d\epsilon_N=d\epsilon_1\cdot a_1^2+d\epsilon_2\cdot a_2^2+d\epsilon_3\cdot a_3^2=\frac{J_3}{J_2}\cdot\left(\frac{d\epsilon_1}{\sigma_1}+\frac{d\epsilon_2}{\sigma_2}+\frac{d\epsilon_3}{\sigma_3}\right)\quad\cdots\cdots(7)$$

$$\frac{d\gamma}{2}=\sqrt{(d\epsilon_1-d\epsilon_2)^2\cdot a_1^2\cdot a_2^2+(d\epsilon_2-d\epsilon_3)^2\cdot a_2^2\cdot a_3^2+(d\epsilon_3-d\epsilon_1)^2\cdot a_3^2\cdot a_1^2}=\frac{J_3}{J_2}\cdot\sqrt{\frac{(d\epsilon_1-d\epsilon_2)^2}{\sigma_1\sigma_2}+\frac{(d\epsilon_2-d\epsilon_3)^2}{\sigma_2\sigma_3}+\frac{(d\epsilon_3-d\epsilon_1)^2}{\sigma_3\sigma_1}}\quad\cdots\cdots(8)$$

Under special conditions of triaxial compression and triaxial extension, τ/σ_N and $d\epsilon_N/d\gamma$ are given respectively by the following equations.

Under triaxial compression condition ($\sigma_2=\sigma_3$ and $d\epsilon_2=d\epsilon_3$):

$$\frac{\tau}{\sigma_N}=\frac{\sqrt{2}}{3}(\sqrt{\sigma_1/\sigma_3}-\sqrt{\sigma_3/\sigma_1})\quad\cdots\cdots(9)$$

$$\frac{d\epsilon_N}{d\gamma}=\frac{\sqrt{\sigma_1/\sigma_3}\cdot d\epsilon_3+\sqrt{\sigma_3/\sigma_1}\cdot(d\epsilon_1/2)}{\sqrt{2}\,(d\epsilon_1-d\epsilon_3)}\quad\cdots\cdots(10)$$

Under triaxial extension condition ($\sigma_1=\sigma_2$ and $d\epsilon_1=d\epsilon_2$):

$$\frac{\tau}{\sigma_N}=\frac{\sqrt{2}}{3}(\sqrt{\sigma_1/\sigma_3}-\sqrt{\sigma_3/\sigma_1})\quad\cdots\cdots(11)$$

$$\frac{d\epsilon_N}{d\gamma}=\frac{\sqrt{\sigma_1/\sigma_3}\cdot(d\epsilon_3/2)+\sqrt{\sigma_3/\sigma_1}\cdot d\epsilon_1}{\sqrt{2}\,(d\epsilon_1-d\epsilon_3)}\quad\cdots\cdots(12)$$

Here, if the basic stress-strain relationships derived from the behavior of soil particles on the mobilized plane and applied to the compounded mobilized planes[2),4)] are also valid for this spatial mobilized plane, then the following equations should hold on the SMP.

$$\frac{\tau}{\sigma_N}=\lambda\cdot\left(-\frac{d\epsilon_N}{d\gamma}\right)+\mu\quad\cdots\cdots(13)$$

$$\frac{\tau}{\sigma_N}=\lambda\cdot\left(-\frac{\epsilon_N}{\gamma}\right)+\mu'\quad(\mu'=\lambda\cdot\bar{\theta}_0+\mu)\quad\cdots\cdots(14)$$

By combining Eqs. (13) and (14) and solving the differential equation, one obtains the following equations.

$$\frac{\tau}{\sigma_N}=(\mu'-\mu)\cdot\ln\frac{\gamma}{\gamma_0}+\mu\quad\cdots\cdots(15)$$

$$\epsilon_N=\frac{\mu-\mu'}{\lambda}\cdot\gamma\cdot\left\{\ln\frac{\gamma}{\gamma_0}-1\right\}\quad\cdots\cdots(16)$$

wherein, the same symbols (λ, μ, μ' and γ_0) as on the compounded mobilized planes are used on the SMP for simplicity. In the above expressions, λ, μ, μ' and γ_0 denote soil parameters which are determined by the kind and state of soil under test. Of these parameters, μ denotes the frictional coefficient between soil particles (=

$\tan\phi_\mu$) and λ is the constant having an approximate value of 1.1-1.5 to be determined by μ. The symbol μ' represents a parameter which has to do with the interparticle friction and the granular structure in the initial state of soil. There are fair indications that under the normal granular structure, these three parameters (λ, μ and μ') may be regarded as assuming approximately constant values for a particular soil specimen. The symbol γ_0 which denotes the value of γ at the maximum compression point of the normal strain ϵ_N on the mobilized plane is believed to form a parameter expressing the granular structure of soil. This is a coefficient which varies with the initial void ratio e_i, the mean effective principal stress σ_m and other factors.

Now, let (a_1, a_2, a_3) and (b_1, b_2, b_3) stand for the direction cosines of the strain increments $d\epsilon_N$ and $d\gamma$ on the SMP respectively, and the conversion of the strain increments $d\epsilon_N$ and $d\gamma$ on the SMP to the respective principal strain increments $d\epsilon_1$, $d\epsilon_2$ and $d\epsilon_3$ will be given by the following equation.

$$d\epsilon_i=d\epsilon_N+\frac{b_i}{a_i}\cdot\frac{d\gamma}{2}\quad(i=1,2,3)\quad\cdots\cdots\cdots\cdots(17)$$

In this equation, a_i is found from Eq. (2) on condition that the direction of the principal stress and that of the principal strain increment are identical. In addition, the direction cosines are of a nature such as to satisfy $b_1^2+b_2^2+b_3^2=1$ and the normality condition gives rise to $a_1\cdot b_1+a_2\cdot b_2+a_3\cdot b_3=0$. One more condition is required because there are three unknowns b_1, b_2 and b_3 while there are two conditional equations. Under the triaxial compression condition, the following equations are evolved from the condition of $b_2=b_3$.

$$\left.\begin{aligned}d\epsilon_1&=d\epsilon_N+\sqrt{2}\cdot\sqrt{\sigma_1/\sigma_3}\cdot\frac{d\gamma}{2}\\ d\epsilon_3&=d\epsilon_N-\frac{1}{\sqrt{2}}\cdot\sqrt{\sigma_3/\sigma_1}\cdot\frac{d\gamma}{2}\end{aligned}\right\}\cdots\cdots\cdots\cdots(18)$$

Since application of $X\equiv\tau/\sigma_N$ to Eqs. (13) and (15) leads to the following equations,

$$d\gamma=\frac{\gamma_0}{\mu'-\mu}\cdot\exp\left(\frac{X-\mu}{\mu'-\mu}\right)\cdot dX$$
$$d\epsilon_N=\frac{\mu-X}{\lambda}\cdot d\gamma$$

Eq. (18) is integrable and the relationship between the principal stresses and the principal strains can be given by the following equations.

$$\left.\begin{aligned}\epsilon_1&=\int_{X=0}^{X=X}d\epsilon_1=\gamma_0\cdot[F_1(X)|_{\text{T.C.}}-F_1(0)|_{\text{T.C.}}]\\ \epsilon_3&=\int_{X=0}^{X=X}d\epsilon_3=\gamma_0\cdot[F_3(X)|_{\text{T.C.}}-F_3(0)|_{\text{T.C.}}]\end{aligned}\right\}\cdots(19)$$

Wherein, $X\equiv\tau/\sigma_N=\dfrac{\sqrt{2}}{3}(\sqrt{\sigma_1/\sigma_3}-\sqrt{\sigma_3/\sigma_1})$

$$F_1(X)|_{\text{T.C.}}=\exp\left(\frac{X-\mu}{\mu'-\mu}\right)\cdot\left\{\frac{9}{16\sqrt{2}}\cdot X^2+\left(\frac{3}{4}-\frac{1}{\lambda}-\frac{9(\mu'-\mu)}{8\sqrt{2}}\right)\cdot X+\frac{1}{\sqrt{2}}+\frac{\mu'}{\lambda}-\frac{3(\mu'-\mu)}{4}+\frac{9(\mu'-\mu)^2}{8\sqrt{2}}\right\}$$

$$F_3(X)|_{\text{T.C.}}=\exp\left(\frac{X-\mu}{\mu'-\mu}\right)\cdot\left\{-\frac{9}{32\sqrt{2}}\cdot X^2+\left(\frac{3}{8}-\frac{1}{\lambda}+\frac{9(\mu'-\mu)}{16\sqrt{2}}\right)\cdot X-\frac{1}{2\sqrt{2}}+\frac{\mu'}{\lambda}-\frac{3(\mu'-\mu)}{8}-\frac{9(\mu'-\mu)^2}{16\sqrt{2}}\right\}$$

It should be noted that approximation is involved in the course of the calculation of this integration. Under the triaxial extension condition, the condition $b_1=b_2$ gives rise to the following equations.

$$\left.\begin{aligned}d\epsilon_1&=d\epsilon_N+\frac{1}{\sqrt{2}}\cdot\sqrt{\sigma_1/\sigma_3}\cdot\frac{d\gamma}{2}\\ d\epsilon_3&=d\epsilon_N-\sqrt{2}\cdot\sqrt{\sigma_3/\sigma_1}\cdot\frac{d\gamma}{2}\end{aligned}\right\}\cdots\cdots\cdots\cdots(20)$$

The following expressions are derived from integrating Eq. (20) similarly to the calculation under the triaxial compression conditions.

$$\left.\begin{aligned}\epsilon_1&=\int_{X=0}^{X=X}d\epsilon_1=\gamma_0\cdot[F_1(X)|_{\text{T.E.}}-F_1(0)|_{\text{T.E.}}]\\ \epsilon_3&=\int_{X=0}^{X=X}d\epsilon_3=\gamma_0\cdot[F_3(X)|_{\text{T.E.}}-F_3(0)|_{\text{T.E.}}]\end{aligned}\right\}\cdots(21)$$

Wherein, $X\equiv\tau/\sigma_N=\dfrac{\sqrt{2}}{3}(\sqrt{\sigma_1/\sigma_3}-\sqrt{\sigma_3/\sigma_1})$

$$F_1(X)|_{\text{T.E.}}=\exp\left(\frac{X-\mu}{\mu'-\mu}\right)\cdot\left\{\frac{9}{32\sqrt{2}}\cdot X^2+\left(\frac{3}{8}-\frac{1}{\lambda}-\frac{9(\mu'-\mu)}{16\sqrt{2}}\right)\cdot X+\frac{1}{2\sqrt{2}}+\frac{\mu'}{\lambda}-\frac{3(\mu'-\mu)}{8}+\frac{9(\mu'-\mu)^2}{16\sqrt{2}}\right\}$$

$$F_3(X)|_{\text{T.E.}}=\exp\left(\frac{X-\mu}{\mu'-\mu}\right)\cdot\left\{-\frac{9}{16\sqrt{2}}\cdot X^2+\left(\frac{3}{4}-\frac{1}{\lambda}+\frac{9(\mu'-\mu)}{8\sqrt{2}}\right)\cdot X-\frac{1}{\sqrt{2}}+\frac{\mu'}{\lambda}-\frac{3(\mu'-\mu)}{4}-\frac{9(\mu'-\mu)^2}{8\sqrt{2}}\right\}$$

Also in this case, approximation is involved in the course of the calculation of the integration. Examination of Eqs. (19) and (21) reveals that the volumetric strain ϵ_v is expressed by the same equation under triaxial compression and triaxial extension conditions alike. Under the plane strain conditions, the following equations are derived from $d\epsilon_2=0$.

$$d\epsilon_1=\frac{a_1^2\cdot d\epsilon_N+\sqrt{a_1^2\cdot a_3^2\cdot(1-a_2^2)\cdot(d\gamma/2)^2-a_1^2\cdot a_2^2\cdot a_3^2\cdot(d\epsilon_N)^2}}{a_1^2\cdot(a_1^2+a_3^2)}$$
$$d\epsilon_3=\frac{a_3^2\cdot d\epsilon_N-\sqrt{a_1^2\cdot a_3^2\cdot(1-a_2^2)\cdot(d\gamma/2)^2-a_1^2\cdot a_2^2\cdot a_3^2\cdot(d\epsilon_N)^2}}{a_3^2\cdot(a_1^2+a_3^2)} \quad \cdots\cdots(22)$$

Where three different principal stresses are exerted, the respective principal strain increments $d\epsilon_1$, $d\epsilon_2$ and $d\epsilon_3$ are given by the following expressions on condition that the direction of τ and that of $d\gamma$ on the SMP are identical.

$$d\epsilon_i=d\epsilon_N+\frac{\sigma_i J_2-3J_3}{\sqrt{J_1J_2J_3-9J_3^2}}\cdot\frac{d\gamma}{2}$$
$$=d\epsilon_N+\frac{\sigma_i-\sigma_N}{\tau}\cdot\frac{d\gamma}{2} \quad (i=1,2,3) \quad \cdots\cdots(23)$$

It follows as a natural consequence that so far as the stress conditions are known, the respective principal strains ϵ_1, ϵ_2 and ϵ_3 can be found by having these principal strain increments integrated along the stress paths. It is also checked that these principal strains calculated from the concept of this spatial mobilized plane agree well with those derived from the former concept of the compounded mobilized planes.

For comparison, a study will be made here with respect to an octahedral plane. Since the direction cosines of the normal of an octahedral plane are $(1/\sqrt{3}, 1/\sqrt{3}, 1/\sqrt{3})$, the shear-normal stress ratio $(\tau/\sigma_N)_{oct}$ and the normal-shear stain increment ratio $(d\epsilon_N/d\gamma)_{oct}$ on this plane are given by the following equations.

$$\left(\frac{\tau}{\sigma_N}\right)_{oct}=\frac{\sqrt{(\sigma_1-\sigma_2)^2+(\sigma_2-\sigma_3)^2+(\sigma_3-\sigma_1)^2}}{\sigma_1+\sigma_2+\sigma_3}=\frac{\tau_{oct}}{\sigma_m} \quad \cdots\cdots(24)$$

$$\left(\frac{d\epsilon_N}{d\gamma}\right)_{oct}=\frac{d\epsilon_1+d\epsilon_2+d\epsilon_3}{2\sqrt{(d\epsilon_1-d\epsilon_2)^2+(d\epsilon_2-d\epsilon_3)^2+(d\epsilon_3-d\epsilon_1)^2}}$$
$$=\frac{d\epsilon_v}{3\cdot d\gamma_{oct}} \quad \cdots\cdots(25)$$

wherein,

$$\tau_{oct}=\frac{1}{3}\sqrt{(\sigma_1-\sigma_2)^2+(\sigma_2-\sigma_3)^2+(\sigma_3-\sigma_1)^2}$$
$$\sigma_m=\frac{1}{3}(\sigma_1+\sigma_2+\sigma_3)$$
$$d\epsilon_v=d\epsilon_1+d\epsilon_2+d\epsilon_3$$
$$d\gamma_{oct}=\frac{2}{3}\sqrt{(d\epsilon_1-d\epsilon_2)^2+(d\epsilon_2-d\epsilon_3)^2+(d\epsilon_3-d\epsilon_1)^2}$$

Under the triaxial compression and triaxial extension conditions alike, Eqs. (24) and (25) are evolved respectively as follows.

$$\left(\frac{\tau}{\sigma_N}\right)_{oct}=\frac{\sqrt{2}}{3}\cdot\frac{(\sigma_1-\sigma_3)}{\sigma_m} \quad \cdots\cdots(26)$$

$$\left(\frac{d\epsilon_N}{d\gamma}\right)_{oct}=\frac{1}{2\sqrt{2}}\cdot\frac{d\epsilon_v}{(d\epsilon_1-d\epsilon_3)} \quad \cdots\cdots(27)$$

The variable $(\sigma_1-\sigma_3)/\sigma_m$ appearing in Eq. (26) and the variable $d\epsilon_v/(d\epsilon_1-d\epsilon_3)$ in Eq. (27) are those which are frequently employed by the Cambridge school and others as parameters to govern the mechanical properties of soil.[6),7)] The question arises as to which set of parameters can more accurately express the properties of soil, those applicable to the octahedral plane or those applicable to the spatial mobilized plane (SMP). This question will be discussed on the basis of test data in the following chapters.

4. VERIFICATION OF PROPOSED EXPRESSIONS BY TEST DATA

4.1 Verification of Relationship between Shear-normal Stress Ratio (τ/σ_N) and Normal-shear Strain Increment Ratio ($d\epsilon_N/d\gamma$) on Spatial Mobilized Plane

In this section, the authors proceed to verify, by using various test data, the basic stress-strain relationships on the spatial mobilized plane and the principal stress-principal strain relationships dealt with in the preceding chapter. As the first step, Eq. (13) indicating the $\tau/\sigma_N-d\epsilon_N/d\gamma$ relationship on the spatial mobilized plane will be discussed. Fig. 2 shows the results of the triaxial compression test ("○" marks: $\sigma_m=1.0$ kg/cm^2 and initial void ratio $e_i=0.889$), the triaxial extension

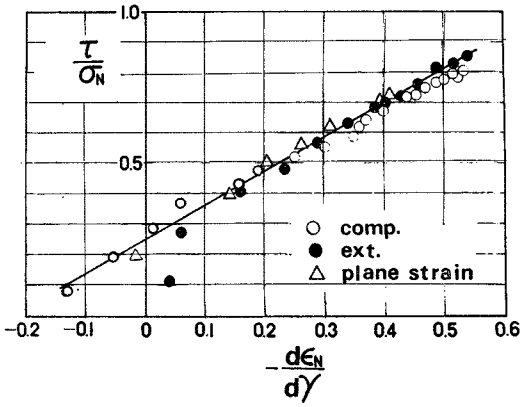

Fig. 2 Relationship between τ/σ_N and $d\epsilon_N/d\gamma$ on spatial mobilized plane in triaxial compression, triaxial extension and plane strain tests on Toyoura sand.

test ("●" marks: σ_m=3.0 kg/cm² and e_i=0.641) and the plane strain test ("△" marks: σ_3=2.0 kg/cm² and e_i=0.663, from Ichihara and Matsuzawa's data[8]) performed on Toyoura sand and analyzed with respect to the $\tau/\sigma_N - d\epsilon_N/d\gamma$ relationship on the spatial mobilized plane (SMP). From this graph, it is seen that the data obtained under the aforementioned three sets of conditions are plotted substantially on the same line. This is an extremely interesting fact which seems to suggest the importance of the physical significance of the spatial mobilized plane (SMP). For the purpose of comparison, the same results of the triaxial compression and triaxial extension tests of Toyoura sand as described above have been analyzed with respect to the $\tau/\sigma_N - d\epsilon_N/d\gamma$ relationship on the octahedral plane in accordance with Eqs. (26) and (27). The results of the analysis are illustrated in Fig. 3. As is evident from this graph, the octahedral plane seems to fail to give a unique interpretation of even the results of triaxial compression and triaxial extension tests. Fig. 4 is a graph obtained by plotting, with respect to the $\tau/\sigma_N - d\epsilon_N/d\gamma$ relationship on the SMP, the results of the plane strain test ("○" marks: $\sigma_1 \cong 1$ kg/cm² and e_i=0.70) and the true triaxial tests ("●" and "△": $\sigma_1 \cong 1$ kg/cm² and e_i=0.71) conducted on dry Toyoura sand subsequent to the K_0-compression performed with a box-type true triaxial apparatus[9] applying the load with rigid plates on all the six planes. Fig. 2 and Fig. 4 clearly indicate that the results of said tests are plotted substantially on the same line in the case of Toyoura sand. The discussion will proceed to the test data of Ottawa sand obtained by Ko and Scott.[10),11] Ko et al. conducted a true triaxial test in which the stress paths were controlled linearly in the radial directions on the octahedral plane having σ_m=1.4 kg/cm² (to be expressed in terms of angular measure of RS which is the abbreviation of radial shear). RS 90° represents a triaxial compression condition and RS 30° a triaxial extension condition respectively, with the angles between the two angles indicating that three different principal stresses are present. Fig. 5 is a graph obtained by plotting the $\tau/\sigma_N - d\epsilon_N/d\gamma$ relationship on the SMP with respect to a relatively loosely packed Ottawa sand. From this graph, it is seen that the results are plotted substantially on the same line

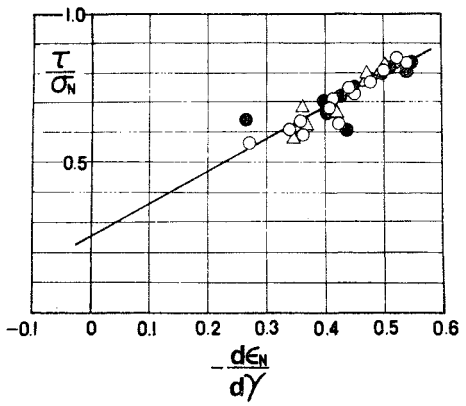

Fig. 4 Relationship between τ/σ_N and $d\epsilon_N/d\gamma$ on spatial mobilized plane in plane strain and true triaxial tests after K_0-compression on Toyoura sand.

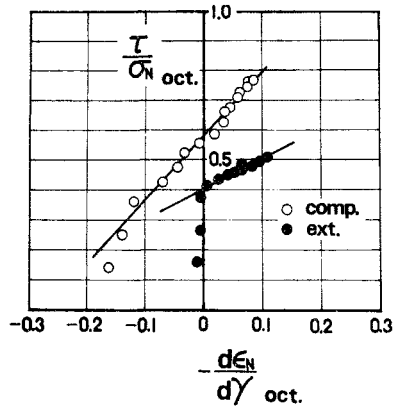

Fig. 3 Relationship between τ/σ_N and $d\epsilon_N/d\gamma$ on octahedral plane in triaxial compression and triaxial extension tests on Toyoura sand.

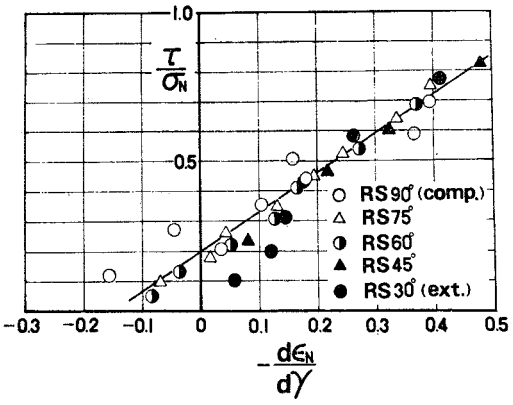

Fig. 5 Relationship between τ/σ_N and $d\epsilon_N/d\gamma$ on spatial mobilized plane in true triaxial tests on Ottawa sand (after Ko and Scott's data).

under stress conditions ranging from those of triaxial compression to those of triaxial extension, though with a slight extent of dispersion in plotting.

The foregoing test data indicate that what the authors designate as "spatial mobilized plane" constitutes an interesting stress plane which provides a unique interpretation of the stress-dilatancy characteristics under three different principal stresses. In accordance with Eq. (13), the ordinate intercepts of the graphs of Figs. 2, 4 and 5 are found to correspond to the interparticle friction coefficients μ and the linear gradients to λ. The values (1.1-1.3) of the linear gradient λ indicated in these graphs are found to be adequate for the values of λ to be calculated with respect to the values (0.20-0.25) of μ.[8]

4.2 Verification of Relationship between Shear-normal Stress Ratio (τ/σ_N) and Normal-shear Strain Ratio (ϵ_N/γ) on SMP

Now, Eq. (14) which represents another basic relationship on the mobilized plane will be discussed. Fig. 6 is a graph obtained by plotting, with respect to the $\tau/\sigma_N-\epsilon_N/\gamma$ relationship on the SMP, the results of three kinds of the same tests on Toyoura sand as those of Fig. 2. Fig. 7 represents a graph obtained by plotting, with respect to the $\tau/\sigma_N-\epsilon_N/\gamma$ relationship on the SMP, the results of five kinds of the same tests on Ottawa sand as those of Fig. 5. These graphs seem to indicate that so long as the data are of the same test specimen, they are plotted approximately on one straight line, different as test conditions may be. In accordance with Eq. (14), the ordinate intercept of this straight line is found

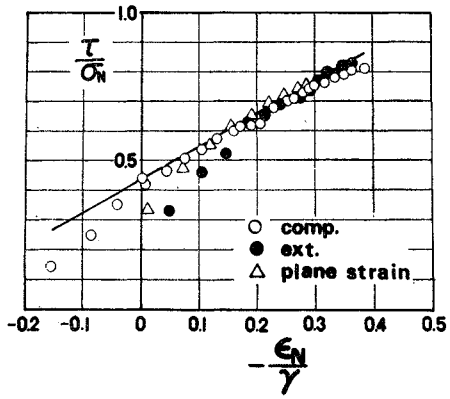

Fig. 6 Relationship between τ/σ_N and ϵ_N/γ on spatial mobilized plane in triaxial compression, triaxial extension and plane strain tests on Toyoura sand.

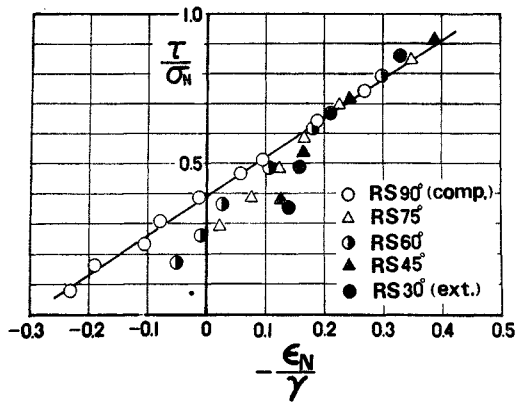

Fig. 7 Relationship between τ/σ_N and ϵ_N/γ on spatial mobilized plane in true triaxial tests on Ottawa sand (after Ko and Scott's data).

to correspond to the values of μ' and the linear gradients to those of λ. From Figs. 2, 4 and 6, the parameters of Toyoura sand are found to be $\lambda=1.1$, $\mu=0.25$ and $\mu'=0.44$. These values are seen to agree essentially with those of λ, μ and μ' obtained of Toyoura sand with respect to the compounded mobilized planes.[2),4)] A possible reason is that the spatial mobilized plane is to the compounded mobilized planes what a resultant plane is to its component planes. From Figs. 5 and 7, the parameters of Ottawa sand are found to be $\lambda=1.3$, $\mu=0.20$ and $\mu'=0.39$.

4.3 Verification of Relationship between Shear-normal Stress Ratio (τ/σ_N), Shear Strain (γ) and Normal Strain (ϵ_N) on SMP

Figs. 8 through 15 show graphs obtained by plotting the test data in accordance with Eqs. (15) and (16). Figs. 8, 9 and 10 represent the curves

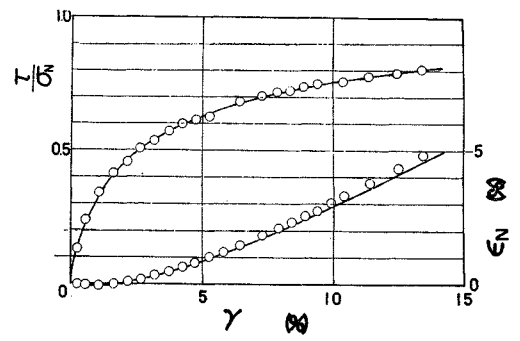

Fig. 8 Relationship among τ/σ_N, γ and ϵ_N on spatial mobilized plane in triaxial compression test on Toyoura sand.

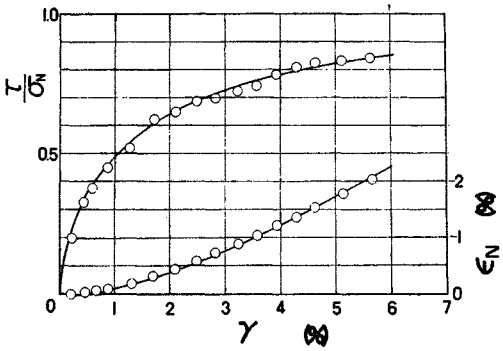

Fig. 9 Relationship among τ/σ_N, γ and ϵ_N on spatial mobilized plane in triaxial extension test on Toyoura sand.

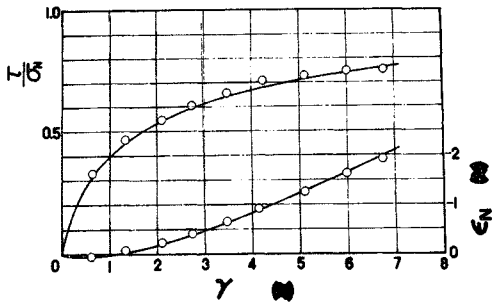

Fig. 10 Relationship among τ/σ_N, γ and ϵ_N on spatial mobilized plane in plane strain test on Toyoura sand (after Ichihara and Matsuzawa's data).

obtained by plotting, with respect to the $\tau/\sigma_N-\gamma-\epsilon_N$ relationship on the SMP, the data of the triaxial compression test (σ_m=1.0 kg/cm² and e_i=0.889), the triaxial extension test (σ_m=3.0kg/cm² and e_i=0.641) and the plane strain test (σ_3=2.0 kg/cm² and e_i=0.663: from Ichihara and Matsuzawa's data[8]) conducted on Toyoura sand and the curves indicating the values calculated from Eqs. (15) and (16). For the calculation, the coefficients λ=1.1, μ=0.25 and μ'=0.44 of Toyoura sand were used. In the case of γ_0, since the initial void ratio and the confining pressure were variable, γ_0=0.70% (Fig. 8), γ_0=0.25% (Fig. 9) and γ_0=0.45% (Fig. 10) were used. The parameter γ_0 on the SMP is a little larger than on the compounded mobilized planes because the former plane is the resultant stress plane of the latter planes. Figs. 11 through 15 represent the curves obtained by plotting, with respect to the $\tau/\sigma_N-\gamma-\epsilon_N$ relationship on the SMP, the five kinds of test data covering triaxial compression to triaxial extension stress conditions of Ottawa sand and

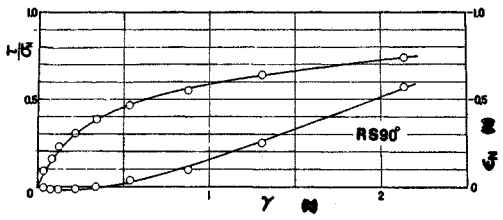

Fig. 11 Relationship among τ/σ_N, γ and ϵ_N on spatial mobilized plane in triaxial compression test (RS 90°) on loose Ottawa sand (after Ko and Scott's data).

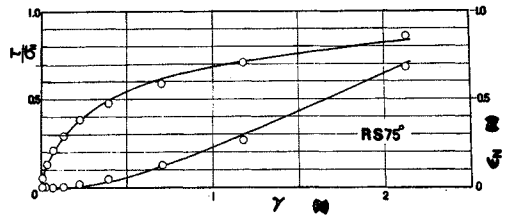

Fig. 12 Relationship among τ/σ_N, γ and ϵ_N on spatial mobilized plane in true triaxial test (RS 75°) on loose Ottawa sand (after Ko and Scott's data).

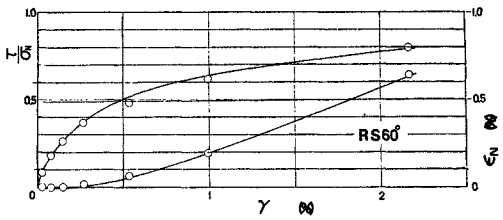

Fig. 13 Relationship among τ/σ_N, γ and ϵ_N on spatial mobilized plane in true triaxial test (RS 60°) on loose Ottawa sand (after Ko and Scott's data).

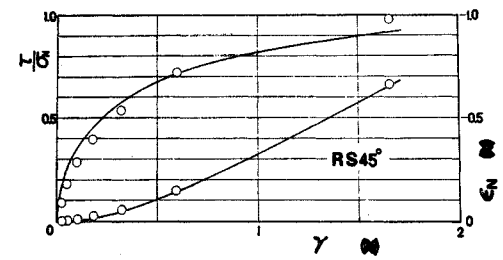

Fig. 14 Relationship among τ/σ_N, γ and ϵ_N on spatial mobilized plane in true triaxial test (RS 45°) on loose Ottawa sand (after Ko and Scott's data).

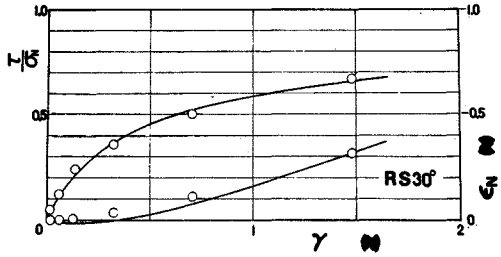

Fig. 15 Relationship among τ/σ_N, γ and ϵ_N on spatial mobilized plane in triaxial extension test (RS 30°) on loose Ottawa sand (after Ko and Scott's data).

the curves indicating the values calculated from Eqs. (15) and (16). For the calculation, the coefficients $\lambda=1.3$, $\mu=0.20$ and $\mu'=0.39$ of Ottawa sand were used. With respect to γ_0, since the initial granular structure differed to some extent, $\gamma_0=0.13\%$ (Fig. 11), $\gamma_0=0.08\%$ (Fig. 12), $\gamma_0=0.10\%$ (Fig. 13), $\gamma_0=0.04\%$ (Fig. 14) and $\gamma_0=0.13\%$ (Fig. 15) were used. Here, these values of γ_0 are determined from the definition that γ_0 is γ at the maximum compression point of the normal strain ϵ_N on the mobilized plane and τ/σ_N equals to μ at $\gamma=\gamma_0$. Though the coefficient γ_0 is considered to serve as a parameter for the evaluation of soil structure, the accurate determination of this parameter is an extremely difficult task. In the elucidation of stress-strain relationships of soil, however, such parameters as involved in the evaluation of soil structure are by all means necessary. It can be expected from comparison of Figs. 11, 12, 13 and 15 that the values of γ_0 are nearly constant under the same mean effective principal stress and the almost same density. (Fig. 14 appears to represent a case in which the structure is slightly more compact than in the other four cases.) It should be noted at this point that, if the initial soil structure is the same, the stress-strain characteristics under three different principal stresses can be uniquely expressed by plotting with respect to the relationships on the spatial mobilized plane.

4.4 Verification of Relationship between Principal Stress Ratios and Principal Strains

Here, the relationship between the principal stress ratios and the principal strains under three different principal stresses as derived through the stress-strain relationships on the spatial mobilized plane will be discussed. Figs. 16, 17 and 18 represent the curves obtained by plotting, with respect to the relationship between the principal stress ratio (σ_1/σ_3) and the principal strains (ϵ_1 and ϵ_3), the data of the triaxial compression test ($\sigma_m=1.0\,\mathrm{kg/cm^2}$ and $e_i=0.889$), the triaxial extension test ($\sigma_m=3.0\,\mathrm{kg/cm^2}$ and $e_i=0.641$) and the plane strain test ($\sigma_3=2.0\,\mathrm{kg/cm^2}$ and $e_i=0.663$: from Ichihara and Matsuzawa's data[8]) on Toyoura sand and the curves indicating the values

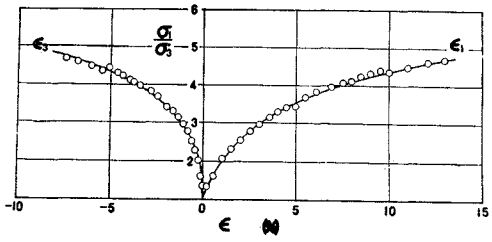

Fig. 16 Relationship among σ_1/σ_3, ϵ_1 and ϵ_3 in triaxial compression test on Toyoura sand.

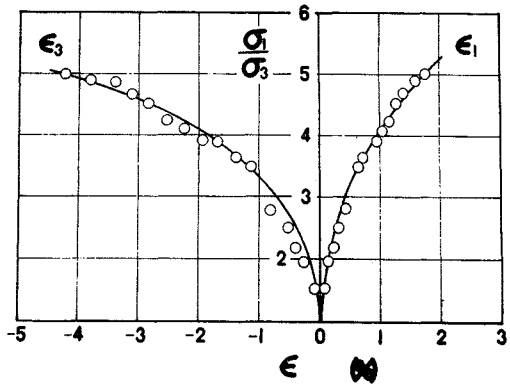

Fig. 17 Relationship among σ_1/σ_3, ϵ_1 and ϵ_3 in triaxial extension test on Toyoura sand.

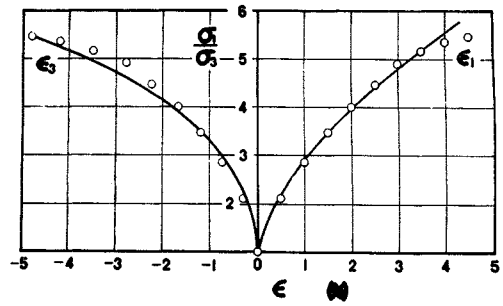

Fig. 18 Relationship among σ_1/σ_3, ϵ_1 and ϵ_3 in plane strain test on Toyoura sand (after Ichihara and Matsuzawa's data).

calculated from Eqs. (19), (21) and (22). For the calculation, the coefficients $\lambda=1.1$, $\mu=0.25$, $\mu'=0.44$ and $\gamma_0=0.70\%$ (Fig. 16), $\gamma_0=0.25\%$ (Fig. 17) and $\gamma_0=0.45\%$ (Fig. 18) were used. Figs. 19 and 20 show the results of the plane strain test ($\sigma_1\cong 1\,kg/cm^2$ and $e_i=0.70$) and those of the true triaxial test ($\sigma_1\cong 1\,kg/cm^2$ and $e_i=0.71$) on dry Toyoura sand subsequent to K_0-compression by use of a box-type true triaxial test apparatus.[9] In the graphs, the curves in solid line are those of the values calculated from Eqs. (22) and (23). Since the shear normally starts from the K_0-compression state in this test apparatus, the curves of calculated values are translated as illustrated in the diagrams to facilitate comparison with the curves of measured values. This translation is based on the idea that the sample in this test apparatus has already been subjected to a magnitude of shear which corresponds to the initial principal stress ratio due to the K_0-compression. For the calculation, the coefficients $\lambda=1.2$, $\mu=0.25$, $\mu'=0.44$ and $\gamma_0=0.23\%$ (Fig. 19) and $\gamma_0=0.18\%$ (Fig. 20) were used. Figs. 21 through 25 represent the curves obtained by plotting, with respect to the relationship between the principal stress ratio (σ_1/σ_3) and the principal strains (ϵ_1, ϵ_2 and ϵ_3), the five kinds of test data covering triaxial compression to triaxial extension stress con-

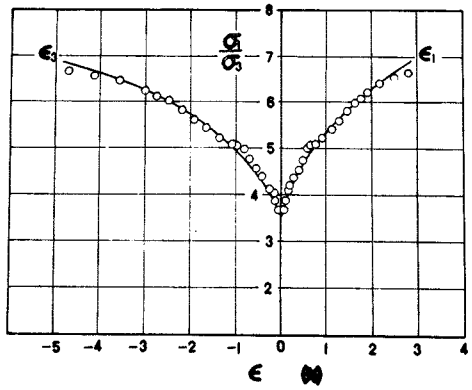

Fig. 19 Relationship among σ_1/σ_3, ϵ_1 and ϵ_3 in plane strain test after K_0-compression on Toyoura sand.

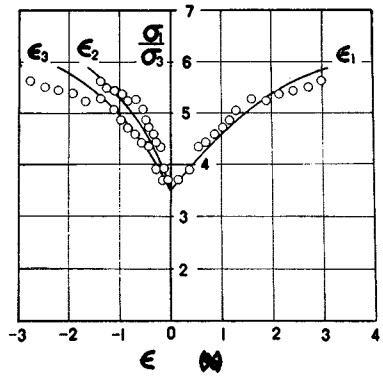

Fig. 20 Relationship among σ_1/σ_3, ϵ_1 and ϵ_3 in true triaxial test after K_0-compression on Toyoura sand.

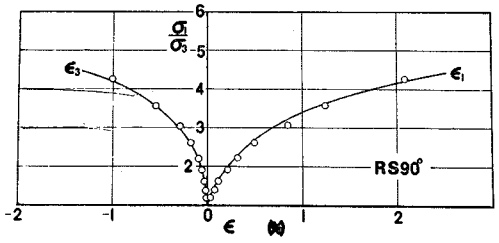

Fig. 21 Relationship among σ_1/σ_3, ϵ_1 and ϵ_3 in triaxial compression test (RS 90°) on loose Ottawa sand (after Ko and Scott's data).

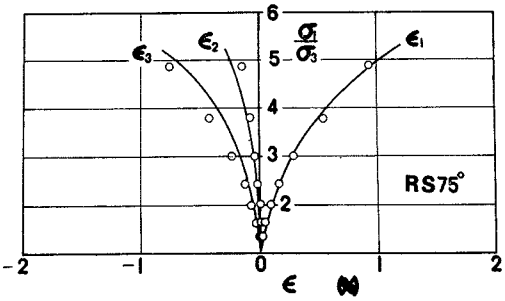

Fig. 22 Relationship among σ_1/σ_3, ϵ_1 and ϵ_3 in true triaxial test (RS 75°) on loose Ottawa sand (after Ko and Scott's data).

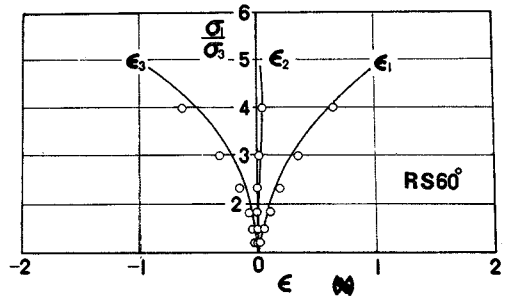

Fig. 23 Relationship among σ_1/σ_3, ϵ_1 and ϵ_3 in true triaxial test (RS 60°) on loose Ottawa sand (after Ko and Scott's data).

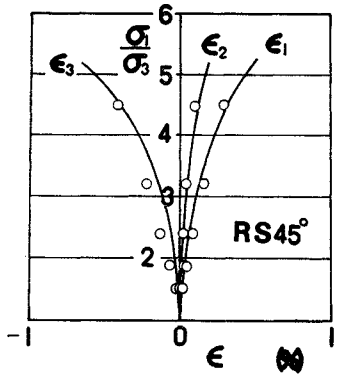

Fig. 24 Relationship among σ_1/σ_3, ϵ_1 and ϵ_3 in true triaxial test (RS 45°) on loose Ottawa sand (after Ko and Scott's data).

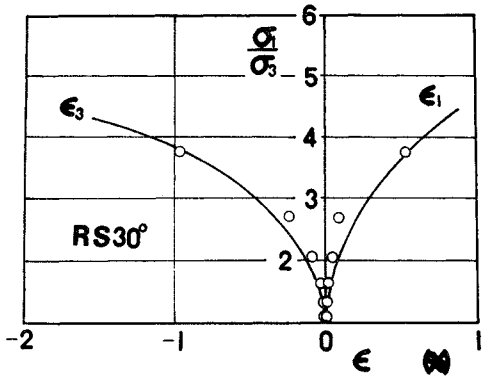

Fig. 25 Relationship among σ_1/σ_3, ϵ_1 and ϵ_3 in triaxial extension test (RS 30°) on loose Ottawa sand (after Ko and Scott's data).

ditions of Ottawa sand and the curves indicating the values calculated from Eq. (23). For the calculation, the coefficients $\lambda=1.3$, $\mu=0.20$, $\mu'=0.39$, $\gamma_0=0.13\%$ (Fig. 21), $\gamma_0=0.08\%$ (Fig. 22), $\gamma_0=0.10\%$ (Fig. 23), $\gamma_0=0.04\%$ (Fig. 24) and $\gamma_0=0.13\%$ (Fig. 25) were used.

From the foregoing results of the tests, the spatial mobilized plane (SMP) proposed in this paper seems to form a stress plane which governs the shear phenomena of soil under three different principal stresses. Thus, deduction of the stress-strain relationship under three different principal stresses through the unique stress-strain relationship on the SMP seems to indicate comprehension of the true nature of soil. It is added that the strains dealt with above are judged to be those ascribable to dilatancy in the light of the idea underlying the derivation of the basic relationships. Strictly speaking, therfore, they should be verified through the constant σ_m test. Here, comparison is made also with the constant σ_3 test and the constant σ_1 test. Since the compressibility of sands is relatively small, satisfactory correspondences are indicated as stated above.

5. PROPOSAL OF NEW YIELD CONDITION

In accordance with Eq. (6), the ratio τ/σ_N on the spatial mobilized plane (SMP) can be transformed as follows:

$$\frac{\tau}{\sigma_N}=\sqrt{\frac{J_1J_2-9J_3}{9J_3}}$$
$$=\frac{2}{3}\sqrt{\frac{(\sigma_1-\sigma_2)^2}{4\sigma_1\sigma_2}+\frac{(\sigma_2-\sigma_3)^2}{4\sigma_2\sigma_3}+\frac{(\sigma_3-\sigma_1)^2}{4\sigma_3\sigma_1}}$$
$$=\frac{2}{3}\sqrt{\tan^2\phi_{12}+\tan^2\phi_{23}+\tan^2\phi_{31}}=K \quad \cdots\cdots(28)$$

On the assumption that soil under test yields when this ratio τ/σ_N on the SMP has reached a fixed value, one can derive the following yield condition (failure criterion).

$$\tan^2\phi_{12}+\tan^2\phi_{23}+\tan^2\phi_{31}$$
$$=\left(\frac{3}{2}K\right)^2=\text{constant} \quad \cdots\cdots(29)$$

The curves in Fig. 26 illustrate Eq. (29) in terms of the relationship between the angle of internal friction $\phi=\phi_{13}=\sin^{-1}\{(\sigma_1-\sigma_3)/(\sigma_1+\sigma_3)\}$ and the parameter $b=(\sigma_2-\sigma_3)/(\sigma_1-\sigma_3)$ indicating the magnitude of the intermediate principal stress σ_2. From this diagram, it is seen that the value of

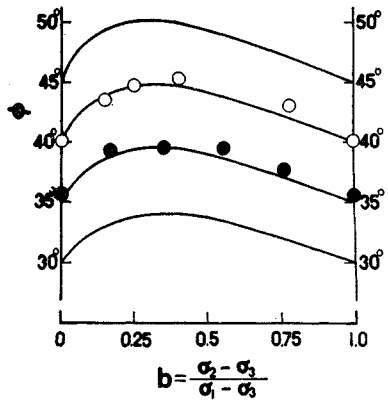

Fig. 26 Proposed yield condition (failure criterion) and measured angles of internal friction of a sand under three different principal stresses (after Sutherland and Mesdary's data).

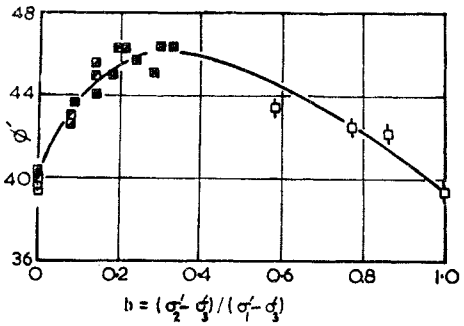

Fig. 27 Measured angles of internal friction of a sand under three different principal stresses (after Ramamurthy and Rawat).

ϕ is equal with respect to $b=0$ (triaxial compression condition) and $b=1$ (triaxial extension condition) and asymmetric with respect to $b=0.5$. The plots given in the diagram represent the results of the test conducted on a certain sand by Sutherland et al.[12] Fig. 27 is intended to give, for the purpose of comparison, the results of the test which Ramamurthy et al.[13] carried out on a sand. It is seen that the curve given in this diagram bears striking resemblance with that of Eq. (29).

Satake,[14] introducing the concept of distance in the stress space, proposes the following yield condition for $n=2$.

$$\left(\frac{\sigma_1-\sigma_2}{\sigma_1+\sigma_2}\right)^2+\left(\frac{\sigma_2-\sigma_3}{\sigma_2+\sigma_3}\right)^2+\left(\frac{\sigma_3-\sigma_1}{\sigma_3+\sigma_1}\right)^2 =\sin^2\phi_{12}+\sin^2\phi_{23}+\sin^2\phi_{31}=2k^2 \quad\cdots\cdots(30)$$

Eqs. (29) and (30) resemble very much in shape each other, except for the difference between $\tan\phi$ and $\sin\phi$. Calculation shows that Eq. (29) gives a slightly larger value of ϕ than Eq. (30), though the difference seems to be limited to within the maximum of 1° where $0°\leqq\phi\leqq45°$. It is, therefore, quite difficult to decide from measured values which gives more realistic yield condition, Eq. (29) or Eq. (30). In such a case as this, the consistency of the theory may be questioned.

Bishop[15] has proposed the following modified equation:

$$\sin\phi=\frac{K_1}{1-K_2\sqrt{b(1-b)}}$$

According to this equation, $\sin\phi$ is symmetric with respect to $b=0.5$ and, therefore, has a fairly different inclination from Eqs. (29) and (30) described above. In this equation, K_1 and K_2 are coefficients which should be determined through experiments.

6. CONCLUSIONS

In the present paper, the authors first proposed a theory that a new stress plane called "spatial mobilized plane" exists within the three-dimensional stress space as a resultant stress plane of the formerly proposed three mobilized planes among the three principal stress axes. They have learnt that the stress-strain relationships of soil under three different principal stresses can be uniquely expressed by analyzing the relationships with respect to this plane. They have derived the equations indicating the principal stress-principal strain relationship in accordance with this unique stress-strain relationship and verified these equations by use of various test data. They have further proposed a new yield condition of soil on the assumption that soil yields when the shear-normal stress ratio on this plane has reached a fixed value. They have demonstrated that this yield condition provides a plausible explanation of the test data.

What the authors wish to stress most in this paper is the fact that the spatial mobilized plane proposed herein forms a stress plane which provides a unique interpretation of the stress-strain characteristics to the yield condition (failure criterion) of soil under three different principal stresses. For the solution of problems concerning deformation and strength of soil, the spatial mobilized plane proves to have an extremely interesting nature. As described briefly in Section 4, such interesting nature may not be expected from the octahedral plane which is frequently resorted to today. This distinction is believed to issue from the physical significance of the mobilized plane, i.e., the plane on which soil particles slide, and the true character of soil as a material fundamentally governed by the frictional law. The authors will aim at analyzing the general stress-strain relationships in tensorial expression through this unique stress-strain characteristics on the spatial mobilized plane.

A description will be made here with respect to the relationship between the spatial mobilized plane (SMP) and the slip plane observed in the soil sample. Since soil is an assemblage of particles, soil particles are considered to slide on the each tangential plane at their contact points along the direction of the resultant shear stress when the resultant shear-normal stress ratio on the tangential plane has reached a fixed value. Therefore, they will not necessarily slide only in the

direction parallel to the intermediate principal stress axis. The SMP may be considered to be the most mobilized plane of soil particles on the average, within the small deformation before the peak strength. On the other hand, the macroscopic slip plane can be observed when the deformation proceed near the residual state. It seems to be probable under the large deformation that the sliding component parallel to the intermediate principal stress axis may increase because soil particles are orientated to the shear direction according to the principal stress ratio. There are no decisive experimental data about this problem, but the slip plane is now investigated by a new true triaxial apparatus. This may be concerned with the fact that von Mises criterion is effective to the metallic materials, though the slip plane occurred in the materials does not always coincide with the octahedral plane.

In closing this paper, the authors wish to express their profound gratitude to Professor Sakuro Murayama of Kyoto University who has rendered warm guidance and assistance for this study. They are also deeply grateful to Professor Masao Satake of Tohoku University, Assistant Professor Daizo Karube of Kobe University and Mr. Tadashi Hashimoto of Osaka Soil Test Laboratory for their useful discussion on the spatial mobilized plane.

REFERENCES

1) Matsuoka, H.: The stress-strain relation of soils under shearing derived from a microscopic consideration, Annuals, Disaster Prevention Research Institute, Kyoto University, No. 15B, 1972, pp. 499-511 (in Japanese).
2) Matsuoka, H.: Stress-strain relationship of soils under three different principal stresses, Annuals, Disaster Prevention Research Institute, Kyoto University, No. 16B, 1973, pp. 711-733 (in Japanese).
3) Matsuoka, H.: A microscopic study on shear mechanism of granular materials, Soils and Foundations, Vol. 14, No. 1, 1974, pp. 29-43.
4) Matsuoka, H.: Stress-strain relationships of sands based on the mobilized plane, Soils and Foundations, Vol. 14, No. 2, 1974, pp. 47-61.
5) Matsuoka, H.: Stress-strain relationships of clays based on the mobilized plane, Soils and Foundations, Vol. 14, No. 2, 1974, pp. 77-87.
6) Roscoe, K. H., A. N. Schofield and A. Thurairajah: Yielding of clays in states wetter than critical, Géotechnique, Vol. 13, 1963, pp. 211-240.
7) Schofield, A. N. and C. P. Wroth: Critical state soil mechanics, McGraw-Hill, London, 1968.
8) Ichihara, M. and H. Matsuzawa: Experiments on shearing characteristics of dry sand under plane strain condition and axial symmetric strain condition, Proc. JSCE, No. 173, 1970, pp. 47-59 (in Japanese).
9) Matsuoka, H. and T. Hashimoto: A newly manufactured true triaxial apparatus and the analysis of its measured data, Proc. Annual Meeting of JSSMFE (8th), 1973, pp. 231-234 (in Japanese).
10) Ko, H. Y. and R. F. Scott: Deformation of sand in shear, Proc. ASCE, Vol. 93, No. SM5, 1967, pp. 283-310.
11) Ko, H. Y. and R. F. Scott: Deformation of sand at failure, Proc. ASCE, Vol. 94, No. SM4, 1968, pp. 883-898.
12) Sutherland, H. B. and M. S. Mesdary: The influence of the intermediate principal stress on the strength of sand, Proc. 7th ICSMFE, Vol. 1, 1969, pp. 391-399.
13) Ramamurthy, T. and R. C. Rawat: Shear strength of sand under general stress system, Proc. 8th ICSMFE, Vol. 1. 2, 1973, pp. 339-342.
14) Satake, M.: A proposal on yield condition of granular materials, Proc. Annual Meeting of JSCE (28th), Part III, 1973, pp. 91-92 (in Japanese).
15) Bishop, A. W.: The strength of soils as engineering materials, Géotechnique, Vol. 16, 1966, pp. 91-130.

(*Received May 23, 1974*)